



ALMA MATER STUDIORUM
UNIVERSITÀ DI BOLOGNA

ARCHIVIO ISTITUZIONALE DELLA RICERCA

Alma Mater Studiorum Università di Bologna Archivio istituzionale della ricerca

Energy and Environmental Performance Comparison of Heat Pump Systems Working with Alternative Refrigerants

This is the final peer-reviewed author's accepted manuscript (postprint) of the following publication:

Published Version:

Energy and Environmental Performance Comparison of Heat Pump Systems Working with Alternative Refrigerants / Dongellini M.; Natale C.; Naldi C.; Rossi di Schio E.; Valdiserri P.; Morini G.L.. - In: APPLIED SCIENCES. - ISSN 2076-3417. - ELETTRONICO. - 13:12(2023), pp. 7238.1-7238.17. [10.3390/app13127238]

Availability:

This version is available at: <https://hdl.handle.net/11585/939760> since: 2023-08-29

Published:

DOI: <http://doi.org/10.3390/app13127238>

Terms of use:

Some rights reserved. The terms and conditions for the reuse of this version of the manuscript are specified in the publishing policy. For all terms of use and more information see the publisher's website.

This item was downloaded from IRIS Università di Bologna (<https://cris.unibo.it/>).
When citing, please refer to the published version.

(Article begins on next page)

Article

Energy and Environmental Performance Comparison of Heat Pump Systems Working with Alternative Refrigerants

Matteo Dongellini, Christian Natale, Claudia Naldi * , Eugenia Rossi di Schio , Paolo Valdiserri 
and Gian Luca Morini 

Department of Industrial Engineering, Alma Mater Studiorum—University of Bologna, Viale del Risorgimento 2, 40136 Bologna, Italy; matteo.dongellini@unibo.it (M.D.); christian.natale3@unibo.it (C.N.); eugenia.rossidischio@unibo.it (E.R.d.S.); paolo.valdiserri@unibo.it (P.V.); gianluca.morini3@unibo.it (G.L.M.)

* Correspondence: claudia.naldi2@unibo.it

Featured Application: An energy and environmental performance analysis of air-source and ground-source heat pump systems able to operate with traditional (R-410A) and alternative low-GWP (R-454B) refrigerants is conducted. The case study is composed of an existing residential single-family house, and the coupled HVAC system is modeled by means of the commercial software TRNSYS. The TEWI index is considered to evaluate the environmental impact of the heat pump systems. The results of the numerical simulations show a significant reduction in the overall greenhouse emissions of those systems in which R-454B is employed as a refrigerant.

Abstract: The European Parliament has imposed to reduce by 2030 whole HFC emissions by at least two-thirds with respect to 2014 levels. With the aim of contributing to determine the energy and environmental advantages of refrigerants alternative to R-410A, this paper reports the results of a numerical study focused on an HVAC system coupled to a residential building and based on a reversible electric heat pump. In particular, two heat pump typologies are considered: an air-source and a ground-source heat pump, both operating with the two refrigerants R-410A and R-454B. The environmental performance of the studied system is assessed by means of the TEWI (total equivalent warming impact) index. The adoption of R-454B involves a slight decrease (2–3%) in the overall annual energy performance of the system with respect to the use of R-410A. On the other hand, the working fluid R-454B guarantees a marked decrease in the TEWI indicator. Indeed, considering the current Italian emission factor of electricity taken from the grid, the total emissions over the entire heat pump operating life drop by about 25% and can decrease by up to 89% in perspective, following the current reduction trend of the emission factor.

Keywords: low-GWP refrigerants; TEWI; seasonal energy performance; R-454B; dynamic simulations



Citation: Dongellini, M.; Natale, C.; Naldi, C.; Rossi di Schio, E.; Valdiserri, P.; Morini, G.L. Energy and Environmental Performance Comparison of Heat Pump Systems Working with Alternative Refrigerants. *Appl. Sci.* **2023**, *13*, 7238. <https://doi.org/10.3390/app13127238>

Academic Editor: Sébastien Poncet

Received: 19 May 2023

Revised: 9 June 2023

Accepted: 14 June 2023

Published: 17 June 2023



Copyright: © 2023 by the authors. Licensee MDPI, Basel, Switzerland. This article is an open access article distributed under the terms and conditions of the Creative Commons Attribution (CC BY) license (<https://creativecommons.org/licenses/by/4.0/>).

1. Introduction

The increase in overall energy demand, combined with the instability of the price of fossil fuels, points out that the use of renewable energy sources is not only a convenient practice but also an absolute priority for the European Union (EU), as recently highlighted by the European Commission through a series of challenging targets set for 2030 [1] and 2050 [2]. In this scenario, heat pumps represent one of the most efficient and promising technologies to reduce greenhouse gas (GHG) emissions linked to civil, industrial and commercial air-conditioning systems [3]. The adoption of HVAC (heating, ventilation and air-conditioning) systems based on electric heat pumps instead of traditional fossil-fuel-based generators offers a series of important advantages, among which it is worth mentioning the integration with renewable-energy-generating systems (e.g., PV panels, solar collectors) [4,5], the simultaneous satisfaction of energy needs related to space heating/cooling and domestic hot water (DHW) production and, finally, the simple integration into pre-existing HVAC systems [6].

In order to further increase the seasonal coefficient of performance (COP) of heat pump systems and decrease their environmental impact, over the last years, particular effort has been paid to the use of alternative refrigerant fluids [7,8]. In particular, Sayyab et al. [7] carried out an experimental analysis on different refrigerants (R513A, R516A, R1234yf and R134a) used in vapor compression cooling and heating systems considering the same steady-state conditions. The authors reported that in cooling mode R513A presented the highest system COP (up to +8%), while R516A showed the lowest system COP at the highest evaporation temperature; however, it exhibited the highest COP and capacity at the lowest evaporation temperature. Ma et al. [8] conducted a comparative analysis on a gas-engine heat pump operating with R152a and R134a, without any changes in lubricant or components; the results showed that using R152a the primary energy ratio increased by 2.6–10.4% and the natural gas consumption rate dropped by 6.0–9.5% with respect to R134a.

Coherently with this research, in the last decades, a series of protocols and regulations have been promulgated to force manufacturers of air-conditioning and refrigeration units to change the adopted refrigerants. As an example, with the Montreal Protocol [9], emanated in 1987, a plan was implemented to progressively phase out the synthetic refrigerants involved in ozone depletion, such as chlorofluorocarbon (CFC) and hydrochlorofluorocarbon (HCFC). Due to the ban of the abovementioned fluids, hydrofluorocarbon (HFC) refrigerants, characterized by a null impact on the ozone layer (ozone depletion potential (ODP) equal to zero), were developed and commercialized [10–12]. Unfortunately, HFCs have a strong environmental impact since their emission in the atmosphere contributes to an increase in global warming.

Since the adoption of the Kyoto Protocol [13], by means of which the joining countries committed a series of interventions to reduce global GHG emissions, the European HVAC market has been continuously influenced by several regulations and protocols aimed at decreasing the environmental impact of air-conditioning and refrigerating units. Currently, the UE protocol 517/2014 [14], known as the “F-gas Regulation”, imposes to reduce by 2030 whole HFC emissions by at least two-thirds with respect to 2014 levels. In order to obtain these outcomes before the prescribed deadline, the regulation has introduced an incremental phasedown of HFC refrigerant fluids, forcing an increasing reduction in the quantity of these fluids that can be commercialized on the market. In addition, strict limits on the mean GWP value of the refrigerants available on the market in the next years have been introduced. As an example, for the 2021–2023 period, the mean GWP value of the refrigerating fluids sold in Europe must be equal to 1035. Additional measures to limit the GHG market have been imposed by the Kigali Amendment (2016) to the Montreal Protocol [15], which outlines a steady 80–85% phaseout of HFCs by the late 2040s.

For all the abovementioned reasons, recently, researchers from both industrial and academic fields have been studying with great interest the development and the use of alternative refrigerants, characterized by lower environmental effects and able to guarantee proper energy performance in HVAC units, such as hydrofluoroolefins (HFOs). Aspects such as environmental impact, safety issues, the replacement of these refrigerants within existent systems and overall energy efficiency have been studied by the scientific community [16]. Currently, refrigerant R-410A is the most widespread fluid within conditioning systems for residential applications, and for this reason, several studies on alternative refrigerants with lower GWP have been conducted over the last years. Among the others, it is worth mentioning the experimental results reported in [17–19]. In particular, Shen and Ally [17] studied the energy and exergy performance of four low-GWP alternative refrigerants (R32, R452B, R454B and R466A) employed in a two-speed air-to-water heat pump and drew conclusions on the corresponding performance to provide space heating in cold climates: the systemic irreversibility of R452B and R454B are consistently lower than that of the other fluids at every compressor speed and external air temperature. Panato et al. [18] developed an experimental setup to evaluate the efficiency of a refrigeration system adopting alternative fluids; under the tested conditions, the R454B fluid had slightly better performance and lower environmental impact than the other nontraditional candidates,

i.e., R452B and R32. Similar experimental results were reported by Sieres et al. [19], who analyzed the working performance of R452B, R454B and R410A. The performance of R454B was similar (heating capacity from -8% to -2% lower, COP values from -0.9% to $+0.6\%$ higher) to that of R410A, with the advantage of a lower optimum refrigerant charge that, combined with a lower GWP, guarantees a significant reduction in direct CO₂ emissions.

In addition, several results on fluids alternative to R410A have been obtained by numerical simulations [20–25]. In particular, Yu et al. [20] performed a theoretical screening of refrigerant mixtures subjected to a multiparameter optimization process consisting of GWP, flammability and thermodynamic parameters; starting from 12 pure refrigerants, the screening identified several mixtures fulfilling all the restrictions, which were promising to be used in applications with a GWP limit below 150. Ghanbarpour et al. [21] provided a global-warming impact analysis of environmentally friendly refrigerants used as replacements for R-134a and R-245fa in medium- and high-temperature heat pumps by considering the emission factors of different countries. The results revealed that in addition to the GWP, the emission factor associated with the sources of electricity generation has a crucial impact on indirect emissions determining whether it is beneficial to employ alternative refrigerants in the heat pump systems. Kong et al. [22] compared the performance of a new-mixture refrigerant, named RHR-1, with commonly used refrigerants including R-134a, R-410A, R-407C and R22, in terms of heating COP, compression ratio and discharging temperature. The new refrigerant, characterized by no ODP and by a GWP of 279, presented a COP in the range of 2.43–4.93, which was higher than other candidates in most design cases. Bellos et al. [23] conducted a parametric investigation of a heat pump operating with R-152A for different operating conditions: various ambient and indoor temperatures and different compressor rotational speeds. Data revealed that R-152A was found to be the most efficient refrigerant compared to natural refrigerants (R-600a and R-290), harmful refrigerants (R-134a and R-404A), as well as promising refrigerants (R32 and R-1234yf). Devecioğlu [24] calculated the seasonal energy performance of heat pumps that utilize alternative refrigerants following the standard EN 14825; R-425B and R-454B resulted as the most suitable fluids among the tested refrigerants. Bobbo et al. [25] carried out a thermodynamic performance analysis, based on energy and exergy balances, of a geothermal heat pump employing either R-410A, R-32 or R-454B refrigerants. The obtained outcomes showed that R-454B was the optimal solution to replace R-410A, leading to a COP increase of up to 5% under different working conditions.

Nevertheless, in the literature, there are still few studies quantifying the energy and environmental advantages of alternative refrigerants for air-source and ground-source heat pump systems. With the aim of contributing to determine the seasonal efficiency and TEWI obtainable with refrigerants alternative to R-410A, in this paper, the results of a numerical study focused on an HVAC system coupled to a residential building and based on a reversible electric heat pump are reported. Both air-source and ground-source heat pumps are taken into account, employed for both winter heating and summer cooling. The main outcomes of this work are the evaluation of the annual energy performance of different heat pump systems, employing the traditional R-410A or the alternative R-454B as refrigerating fluid, in order to show the potential energy and environmental savings linked to the adoption of low-GWP refrigerants.

2. Materials and Methods

2.1. The Building

A residential single-family house built in Padova (north of Italy) in 2018 has been considered in this paper as the application case study. The building is a detached triple-story house and consists of two heated floors and a nonheated attic. In Figure 1, the building 3D model developed in Google SketchUp is shown. The ground floor includes a kitchen, living room, stairwell and bathroom, while on the first floor, three bedrooms, two bathrooms and a stairwell are present. Additionally, a technical room and an unconditioned garage are located on the ground floor. All rooms have a net height of 2.7 m except for the

technical room and garage, which are characterized by a lower height (2.4 m). The total net floor area of the building is about 162 m², while the gross conditioning volume is equal to 705 m³.

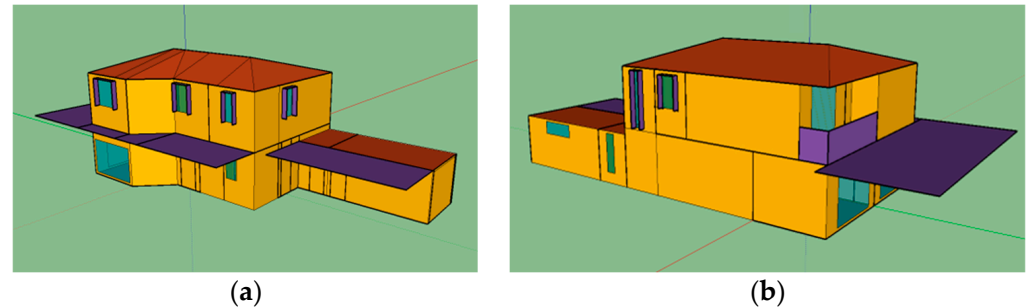


Figure 1. Building 3D model: southwest (a) and northeast (b) view.

The considered residential building is characterized by a high-insulated envelope. Indeed, although it was designed in 2017 and built in 2018, the current demanding limits on transmittance are respected [26]. In particular, the external walls, the slab-on-grade and the roof transmittance values are, respectively, equal to 0.24, 0.14 and 0.24 W m⁻² K⁻¹, while for buildings submitted for energy refurbishment, the standard requires 0.28, 0.29 and 0.24 W m⁻² K⁻¹, respectively. Eleven external windows having a total surface of 33 m² are present in the building. Each window is characterized by low-emissivity double glass (4/12/4) filled with argon. The window frame, made of pliable wood, has a U-value of 1.3 W m⁻² K⁻¹. Consequently, the overall window transmittance is equal to 1.67 W m⁻² K⁻¹. The window solar factor is 0.67, and additionally, internal light-color mobile shields are present.

The tridimensional model of the building has been implemented with Google SketchUp and successively imported within the TRNSYS environment [27]. All features of the building have been defined in the plug-in TRNBuild (Type 56) of TRNSYS, and the numerical model of the HVAC system, reported in Figure 2, has been developed in Simulation Studio. As pointed out in Figure 2, several types from both standard and TESS libraries are included in the model. In particular, Type 534 is used for the thermal energy storage, Type 114 simulates the behavior of single-speed pumps, and Types 647 and 649 are employed for diverters and mixers, respectively. Additionally, the room thermostats are implemented through Type 2d (on-off controller) and are included within macros RT_C (see Figure 2). Specific numerical models introduced by Dongellini and Morini in [28] are used to evaluate the performance of the ASHPs and GCHPs considered in this paper.

In order to define all the elements that influence the energy balance of the building, internal heat gains due to people, equipment and artificial lights have been considered. According to the results of a survey carried out with the building owner, the hourly occupancy profile of the four tenants has been implemented in TRNSYS. The thermal sensible and latent heat emitted per person is equal to 75.5 W and 29 W, respectively, corresponding to a condition of sedentary activity [29]. Regarding the artificial lighting, LED lights are installed in the building's rooms for a total electric power of 724 W. When the lights are switched on, the heat gain is 10% of the total electric power. In this regard, an on-off logic connected to the solar radiation impacting the building's external surfaces has been defined in the numerical model.

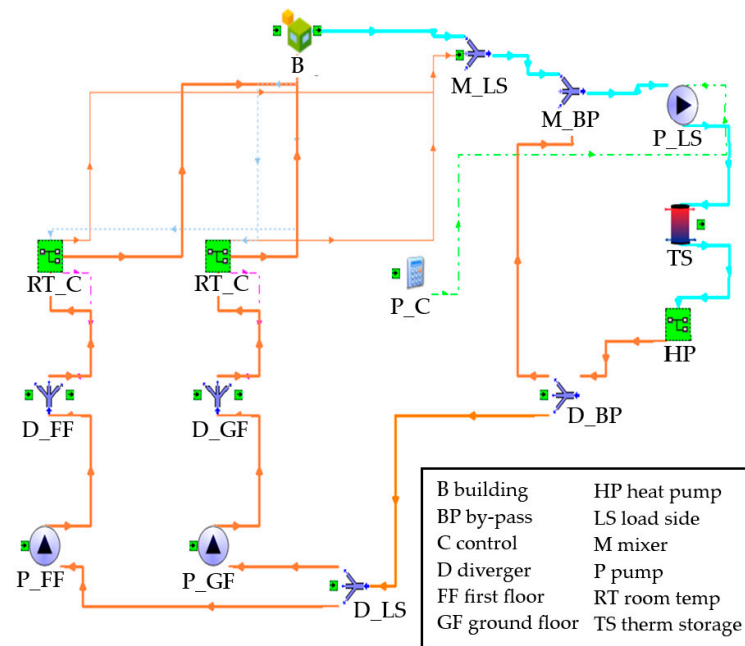


Figure 2. Layout of the complete building–HVAC system model developed in TRNSYS.

2.2. The HVAC System

The HVAC system installed in the building provides space heating and cooling and DHW production. In the present work, the energy consumption linked to the preparation of DHW is not calculated since this part of the system has not been considered in the numerical model.

In Figure 3, the simplified scheme of the whole HVAC system is illustrated.

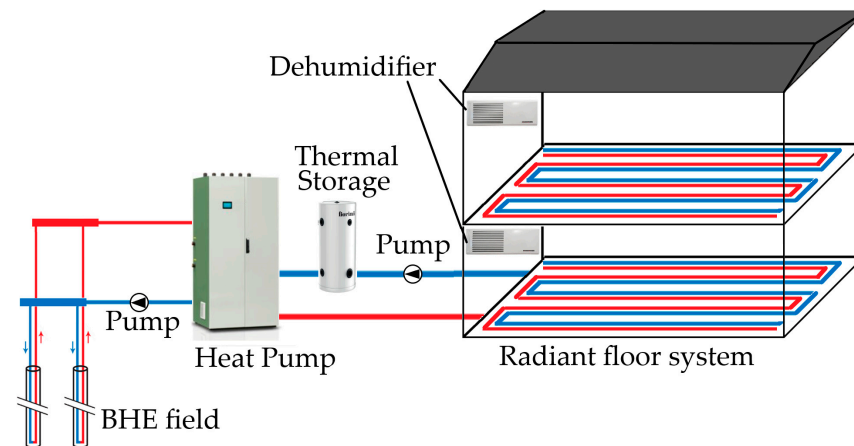


Figure 3. Simplified scheme of the HVAC system dedicated to air-conditioning.

As evident from Figure 3, the system is based on a ground-coupled heat pump (GCHP), coupled to a borehole heat exchanger (BHE) field consisting of two vertical double U-tube boreholes having a depth of 120 m. Each U-tube is 3.7 mm thick, with an external diameter of 40 mm. A mixture of water and 20% ethylenic glycol is used as the heat-carrier fluid in the BHE field. The primary loop (heat pump side) and the secondary loop (user side) are decoupled by a hydraulic separator. In order to increase the thermal inertia of the primary loop, a small thermal storage of 80 L is placed in the heat pump return branch. Two hydraulic pumps are installed in the primary loop. In detail, one circulator (rated electric power input of 75 W) is inserted within the borefield side and the other one (rated electric power input of 47 W) within the load side of the heat pump.

The heat emission system comprises radiant floor surfaces divided into two main loops, one per story. Each loop is composed of a manifold, a circulating pump with a rated absorbed electric power of 13 W and a three-way mixing valve. Each main loop consists of nine separate loops, controlled by means of on–off valves. The radiant floor heating pipes have a pitch of 10 cm. Additionally, a mechanical ventilation unit and a dehumidifying system are installed in the building to provide optimal hygrothermal comfort conditions to the tenants. More in detail, a double-flow-controlled mechanical ventilation system with heat recovery guarantees the renewal of fresh air in all rooms. Finally, in each story of the building, a dehumidifier able to handle an air flow rate of $260 \text{ m}^3 \text{ h}^{-1}$ is installed. The mechanical ventilation system must maintain the conditioned thermal zones to different set-point values, depending on the season. In particular, the set-points are equal to $20 \text{ }^\circ\text{C}$ and $26 \text{ }^\circ\text{C}$ during winter and summer, respectively. On the other hand, internal relative humidity is maintained below 50% throughout the whole year.

As mentioned before, the HVAC system is based on a reversible geothermal heat pump. The generator, placed in the technical room on the ground floor, is a mono-block unit equipped with a BLDC inverter by means of which the compressor rotating speed can be varied continuously. The adopted refrigerant fluid is R-410A, but the heat pump is an “A2L-ready” model able to operate with new refrigerants having lower GWP values and a low inflammability level [30]. Therefore, different fluids can be used with no modifications to the refrigerant cycle components, control logic, lubricating oil, measuring sensors and electric components. Thanks to this peculiarity of the heat pump, the energy and environmental performance of both the traditional fluid R-410A and the alternative fluid R-454B have been investigated by means of dynamic simulations. In Table 1, the main thermophysical properties of the two refrigerants considered in this work are reported.

Table 1. Thermophysical properties of the considered refrigerants.

| Refrigerant | R-410A | R-454B |
|---|-------------------------|----------------------------------|
| Composition (<i>w/w</i>) | R-32: 50% R-125: 50% | R-32: 68.9% HFO-1234yf: 31.1% |
| GWP | 2088 | 457 |
| ODP | 0 | 0 |
| Safety class | A1 | A2L |
| Molar weight (kg/kmol) | 72.6 | 62.6 |
| Critical temperature ($^\circ\text{C}$) | 71.3 | 78.1 |
| Critical pressure (kPa) | 4901 | 5334 |
| Glide (K) | 0.1 | 1.3 |

As evidenced in Table 1, the fluid R-454B is a zeotropic mixture and belongs to the A2L safety class (inflammable with a burning rate less than 10 cm s^{-1}). Indeed, R-454B is one the most promising candidates to replace R-410A in air-conditioning units for buildings since these two fluids have similar thermodynamic properties. As an example, the maximum R-454B condensing pressure is slightly lower than that of R-410A (see Table 1). Moreover, an impactful feature of R-454B is that it can be used as drop-in refrigerant in existing units with the same charge of fluid. Finally, it is important to stress that the R-454B GWP value is 78% lower than that of R-410A, assuring its employment compliant with limits imposed for the near future by the F-gas Regulation.

Figure 4 shows the GCHP characteristic curves in the heating and cooling mode, evaluated at the minimum (30 Hz) and maximum (110 Hz) inverter frequency, as functions of the fluid temperature at the BHE outlet. The heat pump experimental performance data, validated by the manufacturer, are reported for both the refrigerants considered in this analysis. The curves have been obtained considering fixed values of the water temperature at the heat pump inlet/outlet, i.e., $35/40 \text{ }^\circ\text{C}$ and $20/15 \text{ }^\circ\text{C}$ in heating and cooling working modes, respectively. Considering these mentioned criteria and a geothermal fluid temperature at the heat pump inlet/outlet of $4/7 \text{ }^\circ\text{C}$ and $33/28 \text{ }^\circ\text{C}$ in winter and summer, respectively, the heating capacity and the COP of the installed GCHP are equal to 7.4 kW

and 4.85, respectively, while the corresponding values in the summer season are 7.9 kW and 5.7, respectively. In addition, the geothermal fluid temperature difference across the external heat exchanger remains the same whatever refrigerant is adopted.

The heat pump control logic is based on a PID controller, which modulates the inverter working frequency according to the required thermal load, coupled to an on–off controller operating through a hysteresis cycle, characterized by a 5 K dead band. The inverter operating frequency is calculated by comparing the monitored variable, namely the water temperature at the heat pump outlet, with the corresponding set-point value, set to 38 °C during the heating period and to 15 °C in the cooling one. When the minimum inverter frequency is reached and no further modulation is possible under partial load conditions, on–off cycles are performed to modulate the heat pump thermal capacity.

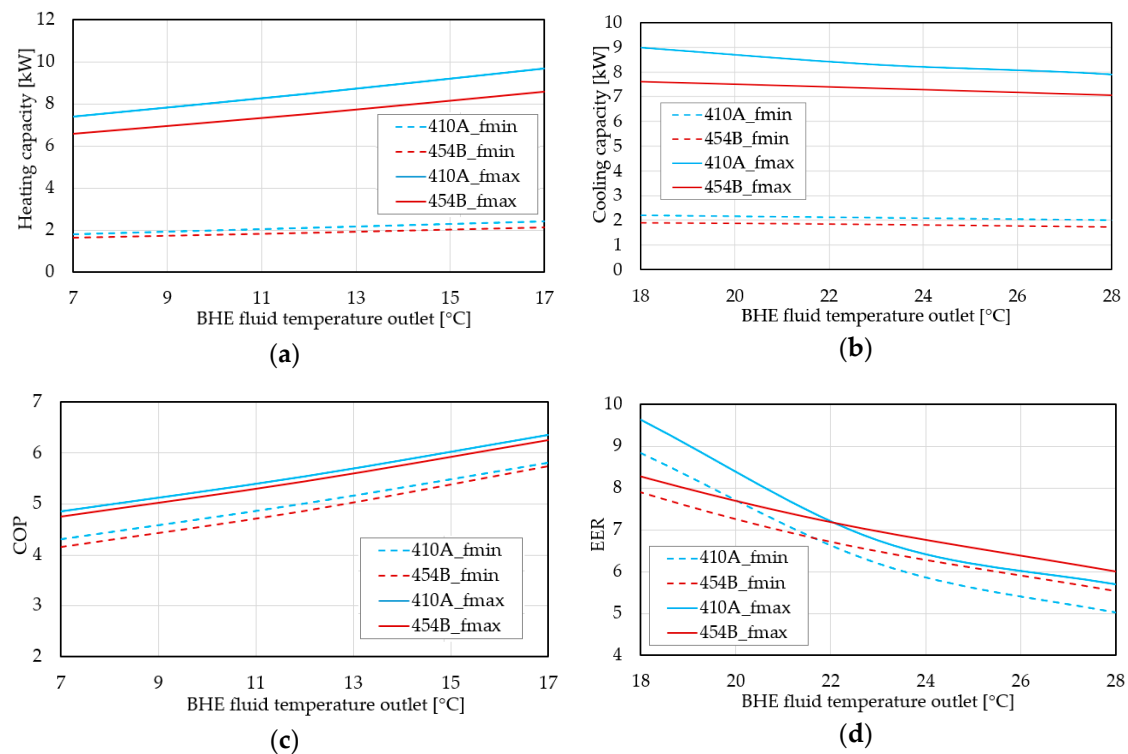


Figure 4. Heating (a) and cooling (b) capacity, COP (c) and EER (d) of the GCHP at the minimum and maximum frequency for R-410A and R-454B.

In order to generalize the findings of this numerical study, an additional heat generator has been considered in this work. In detail, an air-to-water heat pump from the same manufacturer, having the same size as the ground-source unit described before, has been modeled in TRNSYS. Additionally, in this case, the air-source heat pump (ASHP) is an “A2L-ready” unit and can operate with both R-410A and R-454B. Furthermore, it is worth mentioning that the air-source unit is equipped with the same inverter-driven compressor of the GCHP installed in the building and, moreover, is based on the same control logic (i.e., a PID controller to regulate the inverter frequency and on–off controller for the further modulation of the thermal capacity). Therefore, the energy performance of the air-source heat pump, working with the two different refrigerants, has been assessed by means of dynamic simulations and compared to that achieved by the ground-coupled unit in order to investigate the potential energy and environmental savings of R-454B with respect to R-410A for different heat pump typologies. In Figure 5, the characteristic curves of the considered air-source heat pump, evaluated in heating and cooling mode for minimum and maximum inverter frequencies, are reported as functions of the external air temperature for both refrigerants. Reported data have been validated by the manufacturer with experimental tests.

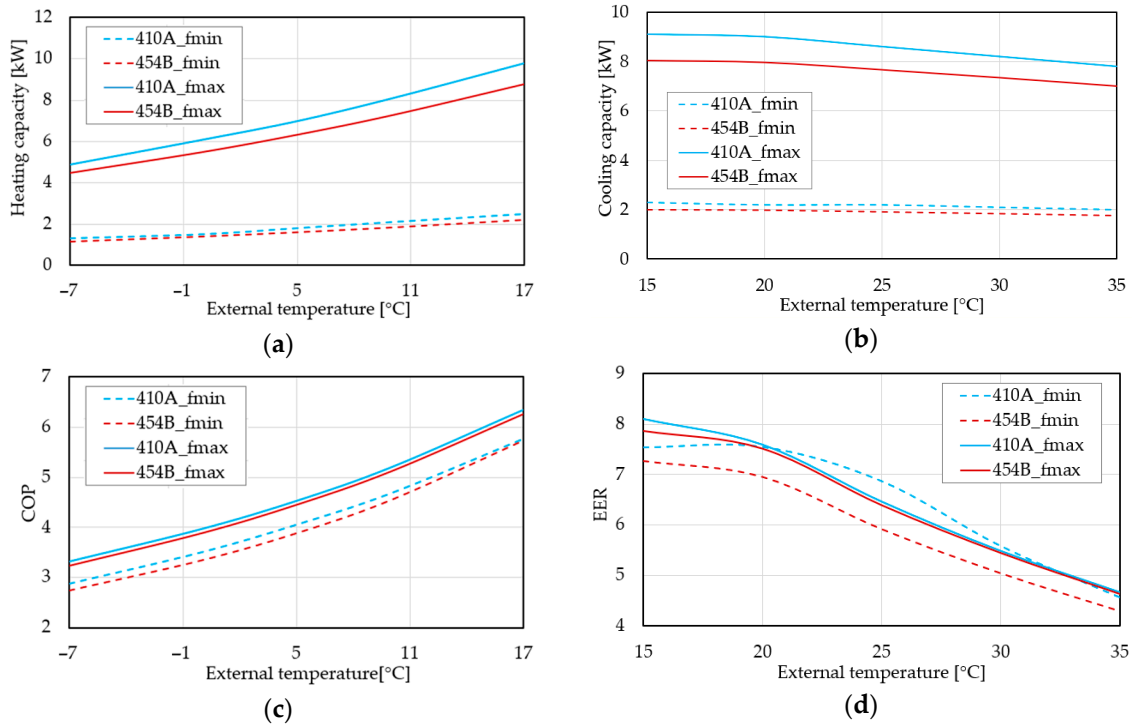


Figure 5. Heating (a) and cooling (b) capacity, COP (c) and EER (d) of the ASHP at the minimum and maximum frequency for R-410A and R-454B.

3. Results and Discussion

3.1. Key Performance Indicators (KPIs)

In this Section, the standard key performance indicators (KPIs) [31] adopted to assess the energy and environmental performance of the four configurations of the HVAC system modeled in TRNSYS are described. First, the energy performance achievable by the system can be calculated on a monthly basis by means of the indicators reported in the following equations:

$$COP_{n,i} = Q_{h,i} / E_{el,compr,i} \tag{1}$$

$$COP_i = Q_{h,i} / (E_{el,compr,i} + E_{el,pump,i}) \tag{2}$$

$$EER_{n,i} = Q_{c,i} / E_{el,compr,i} \tag{3}$$

$$EER_i = Q_{c,i} / (E_{el,compr,i} + E_{el,pump,i}) \tag{4}$$

where $COP_{n,i}$ and $EER_{n,i}$ are the net energy performance coefficients of the heat pump only during the i -th month, COP_i and EER_i are the overall energy performance coefficients of the generating subsystem during the i -th month, which take into account both the heat pump and circulating pump's performance, $Q_{h,i}$ and $Q_{c,i}$ are the thermal energy supplied by the heat pump in heating and cooling mode during the i -th month, respectively, and $E_{el,compr,i}$ and $E_{el,pump,i}$ are the electric energy absorbed by the heat pump compressor and by the circulating pumps coupled to the generator during the i -th month, respectively. As pointed out before, the electric energy need of a single pump is calculated for configurations based on the air-source heat pump, whereas when the ground-source unit is considered, the contribution of two circulators (i.e., borefield side and load side of the heat pump) is taken into account. Finally, it is important to mention that the electric energy consumption of the external heat-exchanger fans for the air-source heat pump is already included in the COP and EER values provided by the manufacturer.

Similarly, it is possible to evaluate the net seasonal energy efficiency of the heat pump ($SCOP_n$ and $SEER_n$) and of the whole HVAC system ($SCOP$ and $SEER$) by means of Equations (5)–(8), where the summations of thermal and electric energy are performed over the entire duration of the heating and cooling periods. More in detail, the heating season ranges from 15 October to 15 April (182 days), while the cooling one ranges from 10 May to 10 September (123 days).

$$SCOP_n = \sum_{i,heat} Q_{h,i} / \sum_{i,heat} E_{el,compr,i} \quad (5)$$

$$SCOP = \sum_{i,heat} Q_{h,i} / \sum_{i,heat} (E_{el,compr,i} + E_{el,pump,i}) \quad (6)$$

$$SEER_n = \sum_{i,cool} Q_{c,i} / \sum_{i,cool} E_{el,compr,i} \quad (7)$$

$$SEER = \sum_{i,cool} Q_{c,i} / \sum_{i,cool} (E_{el,compr,i} + E_{el,pump,i}) \quad (8)$$

Finally, the overall energy efficiency over the entire year can be assessed through the annual performance factor, calculated by Equations (9)–(10) for the heat pump (APF_n) and the entire HVAC system (APF):

$$APF_n = (Q_h + Q_c) / (E_{el,compr,heat} + E_{el,compr,cool}) \quad (9)$$

$$APF = (Q_h + Q_c) / (E_{el,compr,heat} + E_{el,pump,heat} + E_{el,compr,cool} + E_{el,pump,cool}) \quad (10)$$

where Q_h and Q_c are the thermal energy supplied by the heat pump along the entire heating and cooling season, respectively, and $E_{el,compr,heat}$, $E_{el,pump,heat}$, $E_{el,compr,cool}$ and $E_{el,pump,cool}$ are the electric energy absorbed by the heat pump compressor and by the circulating pumps during the heating and cooling season, respectively.

In addition, the TEWI (total equivalent warming impact) index has been selected to study the environmental performance of the studied system configurations. According to its definition in the standard UNI EN 378-1:2021 [32], reported by Equation (11), this indicator allows the consideration of both the direct GHG emissions linked to the refrigerant fluid and the indirect impact connected to the electricity consumption of the air-conditioning unit:

$$TEWI = n \cdot m \cdot GWP \cdot L + m \cdot GWP \cdot (1 - \alpha_{rec}) + n \cdot E_{el} \cdot \beta \quad (11)$$

where n is the heat pump operating life, set to 15 years; m is the refrigerant charge inside the heat pump, equal to 1.2 kg for all the configurations studied in this paper; L is the annual refrigerant leak factor, set equal to 7% [33]; α_{rec} is the refrigerant end-of-life recycle/recovery factor, set to 70% [33]; E_{el} is the overall electric energy consumption of the system and β is the emission factor of the grid electricity. Based on the current available data for the Italian scenario [34], from 2021, the emission factor of the electric energy taken from the grid is equal to 245.7 g_{CO2}/kWh.

3.2. Monthly Energy Performance

Figure 6 compares the monthly energy performance of the HVAC system based on the athermal heat pump and on the geothermal heat pump, by considering R-410A as the refrigerant fluid. Analyzing the obtained results, it is evident that, comparing the KPIs of the heat pump (COP_n and EER_n), the adoption of a GCHP guarantees a significant improvement in generator energy performance with respect to the athermal unit, for both heating and cooling modes. This is reasonable since the ground temperature is always more favorable for the heat pump than the air temperature; it is higher during the heating period and lower during the cooling season, thus enhancing the heat pump's efficiency [35]. Additionally, for both devices, the worst performance is reached in the middle of the conditioning seasons, when the building load is the highest, and the external source temperature is less favorable for the heat pump.

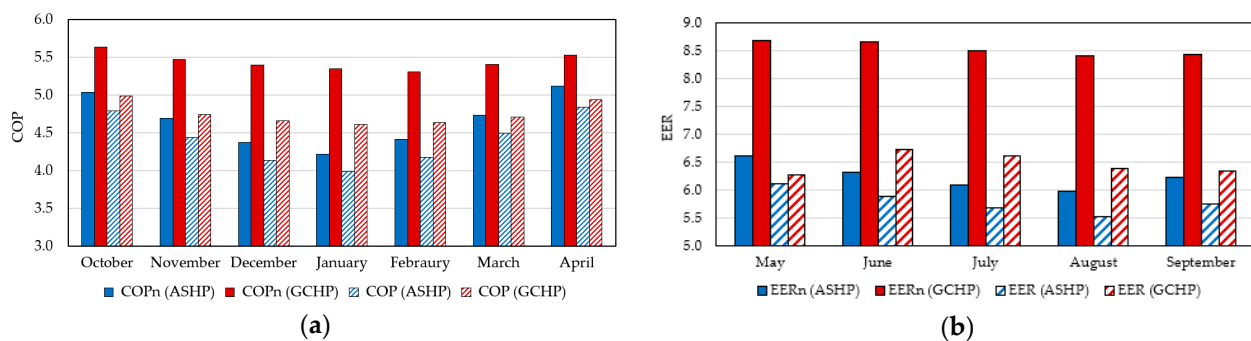


Figure 6. Monthly energy performance of the geothermal and athermal heat pumps with R-410A and of the whole HVAC system in the heating (a) and cooling (b) seasons.

In particular, compared to the first month of the conditioning seasons, the GCHP obtains the worst seasonal efficiency in February (−5.9%) and August (−3.1%), due to the high ground-exploitation rate, while the ASHP obtains the worst seasonal performance in January (−16.3%) and August (−9.5%), when the external air temperature reaches its minimum and maximum values, respectively. Another important aspect highlighted by Figure 6 is that the GCHP efficiency presents a smoother trend across the year (slight monthly performance variations) compared to the ASHP. Indeed, the exploitation of the ground source, characterized by a temperature almost constant over the year, neglects the influence of variable climatic conditions on the heat pump's performance.

Comparing the energy performance of the entire system (KPIs COP and EER), it can be observed that the advantage linked to the adoption of a GCHP is strongly reduced, in particular, during the cooling season (Figure 6b). Indeed, the average summer performance of the GCHP is 39% higher than that of the ASHP, but this percentage reduces to only 15% when the whole HVAC system is considered (heat pump and circulators). From another point of view, the cooling performance of the entire system drops, with respect to that of the heat pump, by 23% with the GCHP and by 7% with the ASHP. In this case, the larger penalization of the overall energy performance of the GCHP system is caused by the energy consumption of the circulating pump installed within the BHE field, which is not present in the athermal configuration. This electric consumption has a higher influence on the seasonal performance factor during summer due to a lower cooling energy request from the building compared to that of the heating period. In other words, the energy need of auxiliaries assumes a more significant influence during the cooling season.

In Figure 7, the energy performance of the HVAC system based on the athermal heat pump is compared to that achieved by the geothermal unit, considering R-454B as the refrigerant fluid.

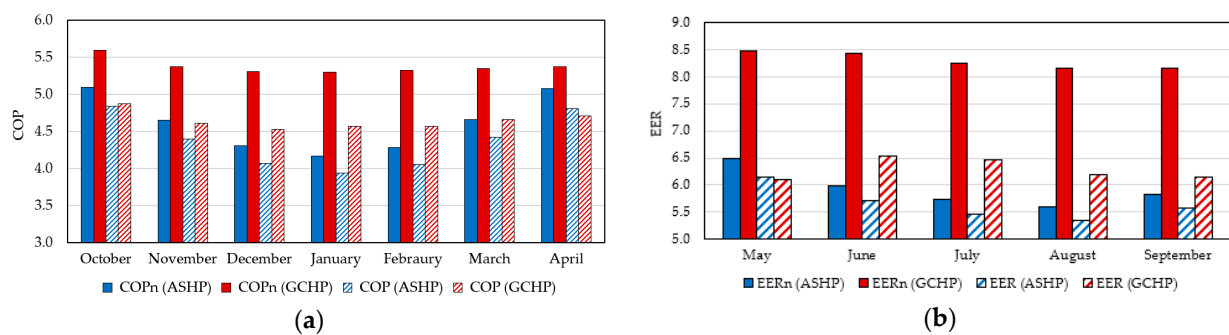


Figure 7. Monthly energy performance of the geothermal and aerothermal heat pumps with R-454B and of the whole HVAC system in the heating (a) and cooling (b) seasons.

According to Figure 7, the performance obtained switching from R410A to R454B is similar to that analyzed previously. Indeed, the GCHP efficiency presents a flatter trend across the months compared to the ASHP, and a huge difference exists between the net energy performance of the heat pump (COP_n , EER_n) and that of the whole HVAC system (COP , EER). Due to the significant monthly variation of ASHP efficiency, the difference in terms of energy performance between ASHP and GCHP changes over the months; it reaches a peak in the middle of the conditioning seasons, when the external air temperature is unfavorable for the air-source unit and the building loads are more relevant, whereas, vice versa, it decreases in the midseasons. As an example, the GCHP COP_n in January is 27% higher than that achieved by the ASHP in the same period, while in April this percentage falls to 6%. Another interesting point revealed by Figure 7 is that in April and May the whole air-source-based system works slightly better than the ground-source one, with a COP and an EER value 2.1% and 0.7% higher, respectively.

3.3. Seasonal Energy Performance and TEWI

In Table 2, a summary of the yearly energy and environmental performance of the studied system configurations is reported as a function of the heat pump typology and refrigerant fluid. If we consider the results of the heat pumps operating with R-410A, it is confirmed that, on a seasonal basis, the heat pump energy performance can be improved by up to 20% in heating mode and even more than 40% in cooling mode when a GCHP is considered, due to the more favorable heat source/sink. However, also taking into account the energy consumption of auxiliaries, the advantage of ground-coupled units drops to 10% and 15%, respectively. Indeed, the overall energy consumption of the circulating pumps increases by about 150%, lowering the global performance of the system. Finally, if the annual performance factor (APF) is considered, it is confirmed that the GCHP has a higher efficiency, with an increase of 25% in this KPI compared to that of the ASHP. In addition, on an annual basis, the advantage of a GCHP-based system is reduced only to 11% when the energy demand of pumps and auxiliaries is considered. It is important to mention that the effective energy penalization mainly depends on the complexity of the hydronic piping, dominant building thermal load among the heating and cooling seasons, operating fluid (pure or glycol water), circulating pump size and its control strategy (fixed-speed, constant or proportional pressure control). For instance, Emmi et al. [36] showed that with a predominant heating load, energy penalization can reach about 12% and 3% in winter and summer, respectively.

On the other hand, analyzing the influence of the adopted refrigerant on the seasonal and annual efficiency, it can be observed that, with the fluid R-454B, a slight decrease in heat pump performance is present and, consequently, in the performance of the entire system. More in detail, the data reported in Table 2 highlight that the performance of the heat pumps operating with R-454B is similar to that achieved with R-410A during the winter period: a slight reduction in $SCOP_n$ is observed, equal to 2%, with both external sources, whereas, considering the auxiliary components, the seasonal efficiency ($SCOP$)

drops by 3% in ground-mode. A slightly greater penalization is noticed during the cooling season. The GCHP and the ASHP $SEER_n$ values drop by about 3% and 6%, respectively; this penalization becomes 3% in both modalities when the auxiliaries ($SEER$) are taken into account. These results are due to a slight drop in heat pump thermal and cooling capacity when the unit operates with the low GWP refrigerant R-454B (see Figures 4 and 5). Indeed, the heat pump operating time rises, and, consequently, the electricity absorbed by the circulating pumps and other auxiliaries increases slightly. More in detail, in winter, the compressor energy consumption increases by about 1%, whereas in summer, this figure rises by 3.5% and 6% for the GCHP and ASHP, respectively. Considering the overall electric consumption, the heat pump system based on R-454B consumes in the heating season 2% and 0.5% more in ground- and air-mode, respectively, while in the cooling season, these values increase to 3% and 6%. To summarize, it is noticed that, on an annual basis, switching from R-410A to R-454B implicates a rise in overall electricity consumption of about 1–2%, with a consequent APF reduction of 2–3%.

Table 2. Energy and environmental performance of the considered HVAC system configurations.

| Refrigerant | R-410A | | R-454B | |
|---|--------|------|--------|------|
| | GCHP | ASHP | GCHP | ASHP |
| Heat pump typology | GCHP | ASHP | GCHP | ASHP |
| Q_h (kWh) | 5280 | 5203 | 5241 | 5145 |
| Q_c (kWh) | 2435 | 2443 | 2438 | 2435 |
| $E_{el,comp,heat}$ (kWh) | 980 | 1162 | 992 | 1166 |
| $E_{el,comp,cool}$ (kWh) | 285 | 398 | 295 | 421 |
| $E_{el,pump,heat}$ (kWh) | 148 | 66 | 159 | 68 |
| $E_{el,pump,cool}$ (kWh) | 87 | 31 | 88 | 32 |
| $SCOP_n$ | 5.39 | 4.48 | 5.28 | 4.41 |
| $SCOP$ | 4.68 | 4.24 | 4.55 | 4.17 |
| $SEER_n$ | 8.53 | 6.14 | 8.26 | 5.79 |
| $SEER$ | 6.54 | 5.70 | 6.36 | 5.53 |
| APF_n | 6.10 | 4.90 | 5.97 | 4.78 |
| APF | 5.14 | 4.62 | 5.00 | 4.53 |
| Direct GHG emissions (kgCO ₂) | 3383 | 3383 | 740 | 740 |
| Indirect GHG emissions (kgCO ₂) | 5738 | 6338 | 5869 | 6453 |
| TEWI (kgCO ₂) | 9120 | 9721 | 6609 | 7193 |

Nevertheless, the analysis of the system environmental performance by means of the TEWI index highlights how the use of a low-GWP refrigerant leads to a significant reduction in GHG emissions across the whole life cycle of the HVAC plant. Although the use of R-454B corresponds to a small increase in indirect emissions, due to the higher electric energy consumption linked to the penalization of heat pump efficiency, the direct emissions of the system decrease dramatically by almost 80%.

As evidenced by Table 2, the adoption of a low-GWP refrigerant allows for the reduction, for both ASHP and GCHP configurations, in CO₂ emissions of about 2500 kg (−26%) over the whole system's life cycle. Another important result is that, in both cases, switching to the fluid with the lower environmental impact, the contribution of indirect emissions grows in relative terms. In fact, indirect GHG emissions represent about 63% of the overall CO₂ emissions in the configurations based on R-410A, while this percentage increases up to 90% adopting R-454B. It is important to mention that the contribution of indirect emissions in the TEWI can be limited in different ways. As an example, the heat pump can be directly powered by PV panels installed on the building; in this way, the electricity absorbed from the grid and thus the indirect emissions would be significantly reduced. Obviously, more efficient heat pump technologies can contribute to reduce electric energy needs and, consequently, indirect GHG emissions. Moreover, taking into account the current energy transition aimed at the complete decarbonization of the electric power system, it is reasonable to expect a continuous drop in the emission factor of the electricity drawn from the grid.

In order to evaluate the expected environmental impact of the studied heat pump systems during the next decades, the TEWI trend associated with the analyzed configurations has been calculated up to 2050, taking into account the upcoming energy transition scenario. The Italian emission coefficient β of the last 30 years has been imported from the Higher Institute for Environmental Protection and Research (ISPRA) database [34]. The analysis of the reported data outlines that the value of β was more than halved from 1990 to 2020, decreasing from $577.9 \text{ gCO}_2 \text{ kWh}^{-1}$ to $255 \text{ gCO}_2 \text{ kWh}^{-1}$, thanks to a deep penetration of renewable energy sources into the national energy mix. In addition, a decreasing trend in the emission factor has been estimated during the next years on the basis of the ambitious European goals set by the European Green Deal [2], aimed at the complete decarbonization of the energy sector by 2050. In particular, the emission factor in 2050 has been considered null, and its reduction with respect to the value of 2020 has been set equal to 15%, 33%, 50%, 66% and 85% for the years 2025, 2030, 2035, 2040 and 2045, respectively. In order to clarify, the β values during the analyzed years are reported in Table 3.

Table 3. Values of the emission coefficient β expected for the next years.

| Year | 2025 | 2030 | 2035 | 2040 | 2045 | 2050 |
|--|-------|-------|-------|------|------|------|
| $\beta \text{ [gCO}_2 \text{ kWh}^{-1}]$ | 216.8 | 170.9 | 127.5 | 86.7 | 38.3 | 0 |

Figure 8 shows the trend of TEWI for the HVAC system based on the GCHP operating with R-410A (Figure 8a) and R-454B (Figure 8b), with the share of direct and indirect emissions out of the total. From the graphs of Figure 8, it is evident that the value of TEWI has been monotonically decreasing for years, for both refrigerants, since a drop in the electricity emission factor causes a significant reduction in the indirect emissions of the system. In particular, compared to the situation in 2020, by the year 2050, the overall CO₂ emissions drop by 63% and 89% in the R-410A and R-454B systems, respectively. A significant outcome for both refrigerants is that, in the analyzed scenario, the share of direct emissions becomes more and more important with respect to indirect emissions, in agreement with the electricity emission-factor trend.

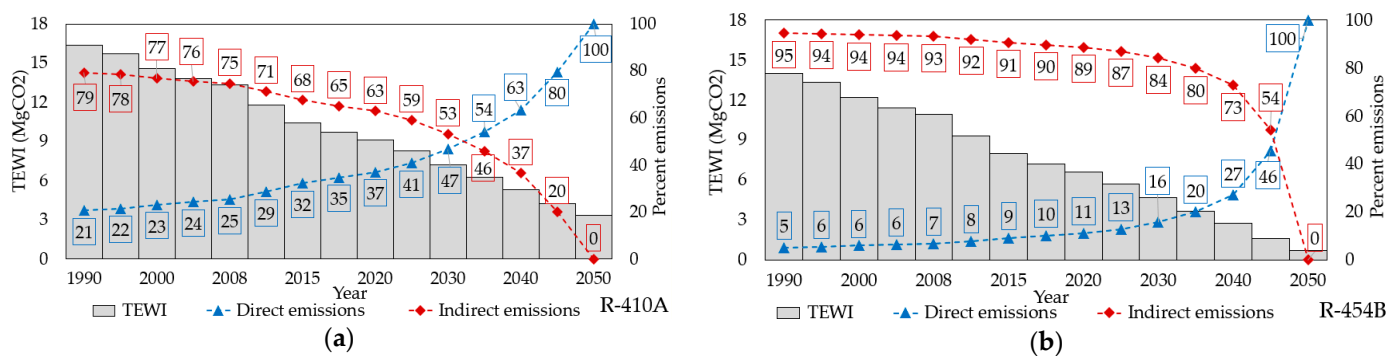


Figure 8. Trend of TEWI and contributions of direct/indirect emissions expected for the next years for the GCHP-based system operating with R-410A (a) and R-454B (b).

More in detail, from Figure 8a, it is evident that for traditional refrigerants, such as R-410A, the weight of direct emissions increased from 21% in 1990 to 37% in 2020, highlighting how the adoption of more environmental-friendly fluids, characterized by lower GWP values imposed by the current regulation, is essential to improve the sustainability of air-conditioning systems. Indeed, the comparison of Figure 8a,b points out that it is possible to strongly reduce the overall environmental impact with R-454B since the contribution of indirect emissions will become negligible with respect to that of direct emissions in the next years. As an example, direct emissions are expected to represent the totality of the system's GHG emissions in 2050.

In order to complete the overview of the environmental performance of the studied configurations, the TEWI trend related to the ASHP-based system is illustrated in Figure 9. Comparing Figures 8 and 9, it is clear that the contribution of direct/indirect emissions out of the total remains almost the same even in the case of aerothermal units. Indeed, compared to the GCHP, the rise in the annual electric consumption of the ASHP systems weakly increases the weight of indirect emissions by about 2.5% for both refrigerants.

Another interesting aspect is that when R-454B is used, the indirect emissions share remains stable for a prolonged time (up to 2040) before plunging, whereas when R-410A is adopted, the indirect emissions share constantly decreases. This trend for R-410A mostly depends on the large weight of the direct emissions and thus on the high R-410A GWP value. Finally, the results confirm that in the next years the share of direct emissions will be predominant, and thus the switch to eco-friendly low-GWP fluids will be necessary to accomplish the European targets.

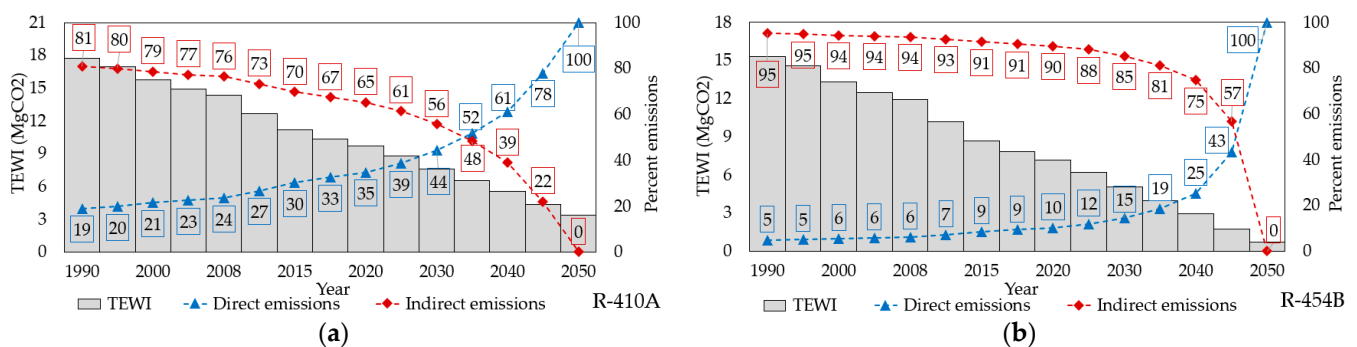


Figure 9. Trend of TEWI and contributions of direct/indirect emissions expected for the next years for the ASHP-based system operating with R-410A (a) and R-454B (b).

4. Conclusions

In this paper, the environmental and energy performance of different configurations of a heat-pump-based air-conditioning system, coupled to a single-family building, has been evaluated numerically as a function of the heat pump typology and of the refrigerant fluid. The numerical model of the building and the analyzed system configurations have been implemented within the dynamic simulation software TRNSYS. In particular, a ground-coupled and an air-source heat pump, having the same size and built by the same manufacturer, have been considered. Both units can operate with two different refrigerants: R-410A and its low-GWP alternative R-454B.

The analysis of the seasonal and annual energy performance of the studied configurations of the HVAC system points out that the annual energy efficiency can be increased by 25% using a geothermal heat pump in place of a similar air-source model. Nevertheless, this advantage is more than halved, decreasing to 11%, if the electric energy consumption of the circulating pumps is also taken into account to calculate the seasonal performance factor of the whole air-conditioning system. Indeed, the contribution of auxiliaries to the overall electric consumption of heat pump systems cannot be negligible, especially under partial building loads. It is important to emphasize that the actual energy penalization depends on the complexity of the hydronic loop and the circulating pump's dimension and working modality (fixed-speed, constant or proportional pressure control). Additionally, numerical results show that the annual overall energy performance of the system is slightly reduced by 2–3% when the fluid R-454B is adopted in place of R-410A. Due to the thermophysical properties of the low-GWP refrigerant, the net penalization rises up to 6% during the cooling period.

On the other hand, it has been demonstrated, by means of the TEWI index, that the use of R-454B allows to significantly reduce the global environmental impact of the system in terms of CO₂ emissions across its whole life cycle. Although the indirect emissions linked to configurations based on R-454B minimally increase, due to the slight penalization of the

heat pump's efficiency, the direct emissions are strongly reduced. Furthermore, although the overall electric consumption rises in ASHP systems, the share of indirect emissions remains almost the same with respect to GCHP systems, slightly increasing by 2.5%. The overall CO₂ emissions are generally reduced by about 26% with the low-GWP refrigerant, and this percentage will become further relevant in the next years when the emission factor of electric energy taken from the grid will significantly drop thanks to a wider penetration of renewable sources in the energy sector. In the next decades, when power production will be decarbonized, the environmental impact of air-conditioning systems will be linked to the direct emissions of refrigerants, and thus the use of low- or very-low-GWP fluids must be pursued and mandatorily promoted by future regulations.

Author Contributions: Conceptualization, M.D. and G.L.M.; methodology, M.D. and C.N. (Claudia Naldi); software, M.D. and C.N. (Christian Natale); validation, M.D. and C.N. (Claudia Naldi); formal analysis, G.L.M., P.V. and E.R.d.S.; investigation, M.D. and C.N. (Claudia Naldi); resources, C.N. (Christian Natale) and E.R.d.S.; data curation, C.N. (Christian Natale); writing—original draft preparation, C.N. (Christian Natale); writing—review and editing, M.D. and C.N. (Claudia Naldi); visualization, P.V. and E.R.d.S.; supervision, G.L.M.; project administration, G.L.M.; funding acquisition, G.L.M. and C.N. (Claudia Naldi). All authors have read and agreed to the published version of the manuscript.

Funding: The research leading to these results has received funding from the Italian Ministry of University and Research (MUR) within the framework of the PRIN2017 project «The energy FLEXibility of enhanced HEAT pumps for the next generation of sustainable buildings (FLEXHEAT)», grant 2017KAAECT and from PNRR—Missione 4—Componente 2, Investimento 1.5 Creazione e rafforzamento di Ecosistemi dell'innovazione, costruzione di leader territoriali di R&S D.D. 3277 del 30/12/2021, under the research project ECOSISTER-Ecosystem for Sustainable Transition in Emilia-Romagna (Spoke N. 4—Smart mobility, housing and energy solutions for a carbon-neutral society), Code ECS00000033, CUP J33C22001240001.

Institutional Review Board Statement: Not applicable.

Informed Consent Statement: Not applicable.

Data Availability Statement: Data available on request due to restrictions privacy.

Conflicts of Interest: The authors declare no conflict of interest.

Nomenclature

| | |
|---------------|---|
| L | annual refrigerant leak factor (%) |
| m | refrigerant charge (kg) |
| n | heat pump operating life (year) |
| E_{el} | electric energy (kWh) |
| Q | thermal energy (kWh) |
| Abbreviations | |
| APF | annual performance factor |
| ASHP | air-source heat pump |
| BHE | borehole heat exchanger |
| COP | coefficient of performance |
| DHW | domestic hot water |
| EER | energy efficiency ratio |
| GCHP | ground-coupled heat pump |
| GHG | greenhouse gas emission |
| GWP | global warming potential |
| HVAC | heating, ventilation and air-conditioning |
| KPI | key performance indicator |
| ODP | ozone depletion potential |
| SCOP | seasonal coefficient of performance |

| | |
|----------------|---|
| SEER | seasonal energy efficiency ratio |
| TEWI | total equivalent warming impact (kgCO ₂) |
| Greek symbols | |
| α_{rec} | refrigerant end-of-life recovery factor (%) |
| β | emission factor of grid electricity (gCO ₂ /kWh) |
| Subscripts | |
| <i>c</i> | cooling |
| <i>compr</i> | compressor |
| <i>cool</i> | cooling season |
| <i>h</i> | heating |
| <i>heat</i> | heating season |
| <i>i</i> | <i>i</i> -th month |
| <i>n</i> | net |
| <i>pump</i> | circulating pump |

References

1. European Commission. *2030 Climate & Energy Framework*; European Commission: Brussels, Belgium, 2020.
2. European Commission. *The European Green Deal*; European Commission: Brussels, Belgium, 2019.
3. Dongellini, M.; Naldi, C.; Morini, G.L. Seasonal performance evaluation of electric air-to-water heat pump systems. *Appl. Therm. Eng.* **2015**, *90*, 1072–1081. [[CrossRef](#)]
4. Kaygusuz, K.; Ayhan, T. Experimental and theoretical investigation of combined solar heat pump system for residential heating. *Energy Convers. Manag.* **1999**, *40*, 1377–1396. [[CrossRef](#)]
5. Lazzarin, R.M. Dual source heat pump system: Operation and performance. *Energy Build.* **2012**, *52*, 77–85. [[CrossRef](#)]
6. Montero, O.; Brischoux, P.; Callegari, S.; Fraga, C.; Rüetschi, M.; Vionnet, E.; Calame, N.; Rognon, F.; Patel, M.; Hollmuller, P. Large Air-to-Water Heat Pumps for Fuel-Boiler Substitution in Non-Retrofitted Multi-Family Buildings—Energy Performance, CO₂ Savings, and Lessons Learned in Actual Conditions of Use. *Energies* **2022**, *15*, 5033. [[CrossRef](#)]
7. Al-Sayyab, A.K.S.; Navarro-Esbri, J.; Barragan-Cervera, A.; Kim, S.; Mota-Babiloni, A. Comprehensive experimental evaluation of R1234yf-based low GWP working fluids for refrigeration and heat pumps. *Energy Convers. Manag.* **2022**, *258*, 115378. [[CrossRef](#)]
8. Ma, Z.; Liu, F.; Tian, C.; Jia, L.; Wu, W. Experimental comparisons on a gas engine heat pump using R134a and low-GWP refrigerant R152a. *Int. J. Refrig.* **2020**, *115*, 73–82. [[CrossRef](#)]
9. United Nations. *The Montreal Protocol on Substances that Deplete the Ozone Layer*; United Nations: Montreal, QC, Canada, 1987.
10. Rigby, M.; Prinn, R.G.; O'Doherty, S.; Miller, B.R.; Ivy, D.; Mühle, J.; Harth, C.M.; Salameh, P.K.; Arnold, T.; Weiss, R.F.; et al. Recent and future trends in synthetic greenhouse gas radiative forcing. *Geophys. Res. Lett.* **2014**, *41*, 2623–2630. [[CrossRef](#)]
11. O'Doherty, S.; Rigby, M.; Mühle, J.; Ivy, D.J.; Miller, B.R.; Young, D.; Simmonds, P.G.; Reimann, S.; Vollmer, M.K.; Krummel, P.B.; et al. Global emissions of HFC-143a (CH₃CF₃) and HFC-32 (CH₂F₂) from in situ and air archive atmospheric observations. *Atmos. Chem. Phys.* **2014**, *14*, 9249–9258. [[CrossRef](#)]
12. Velders, G.J.M.; Fahey, D.W.; Daniel, J.S.; McFarland, M.; Andersen, S.O. The large contribution of projected HFC emissions to future climate forcing. *Proc. Natl. Acad. Sci. USA* **2009**, *106*, 10949–10954. [[CrossRef](#)]
13. United Nations. *Kyoto Protocol to the United Nations Framework Convention on Climate Change*; United Nations: Kyoto, Japan, 1997.
14. European Parliament. *Regulation (EU) N° 517/2014 of the European Parliament and of the Council of 16 April 2014 on Fluorinated Greenhouse Gases and Repealing Regulation (EC) No 842/2006*; European Parliament: Brussels, Belgium, 2014.
15. United Nations. *Amendment to the Montreal Protocol on Substances that Deplete the Ozone Layer*; United Nations: Kigali, Rwanda, 2016.
16. Yang, Z.; Feng, B.; Ma, H.; Zhang, L.; Duan, C.; Liu, B.; Zhang, Y.; Chen, S.; Yang, Z. Analysis of lower GWP and flammable alternative refrigerants. *Int. J. Refrig.* **2021**, *126*, 12–22. [[CrossRef](#)]
17. Shen, B.; Ally, M.R. Energy and Exergy Analysis of Low-Global Warming Potential Refrigerants as Replacement for R410A in Two-Speed Heat Pumps for Cold Climates. *Energies* **2020**, *13*, 5666. [[CrossRef](#)]
18. Panato, V.H.; Marcucci Pico, D.F.; Bandarra Filho, E.P. Experimental evaluation of R32, R452B and R454B as alternative refrigerants for R410A in a refrigeration system. *Int. J. Refrig.* **2022**, *135*, 221–230. [[CrossRef](#)]
19. Sieres, J.; Ortega, I.; Cerdeira, F.; Álvarez, E. Drop-in performance of the low-GWP alternative refrigerants R452B and R454B in an R410A liquid-to-water heat pump. *Appl. Therm. Eng.* **2021**, *182*, 116049. [[CrossRef](#)]
20. Yu, B.; Ouyang, H.; Shi, J.; Liu, W.; Chen, J. Evaluation of low-GWP and mildly flammable mixtures as new alternatives for R410A in air-conditioning and heat pump system. *Int. J. Refrig.* **2021**, *121*, 95–104. [[CrossRef](#)]
21. Ghanbarpour, M.; Mota-Babiloni, A.; Badran, B.E.; Khodabandeh, R. Theoretical Global Warming Impact Evaluation of Medium and High Temperature Heat Pumps Using Low GWP Refrigerants. *Appl. Sci.* **2021**, *11*, 7123. [[CrossRef](#)]
22. Kong, X.; Zhang, Y.; Nie, J. A New Mixture Refrigerant for Space Heating Air Source Heat Pump: Theoretical Modelling and Performance Analysis. *Appl. Sci.* **2018**, *8*, 622. [[CrossRef](#)]
23. Bellos, E.; Tzivanidis, C. Investigation of the Environmentally-Friendly Refrigerant R152a for Air Conditioning Purposes. *Appl. Sci.* **2019**, *9*, 119. [[CrossRef](#)]

24. Devecioğlu, A.G. Seasonal performance assessment of refrigerants with low GWP as substitutes for R410A in heat pump air conditioning devices. *Appl. Therm. Eng.* **2017**, *125*, 401–411. [[CrossRef](#)]
25. Bobbo, S.; Fedele, L.; Curcio, M.; Bet, A.; De Carli, M.; Emmi, G.; Poletto, F.; Tarabotti, A.; Mendrinòs, D.; Mezzasalma, G.; et al. Energetic and Exergetic Analysis of Low Global Warming Potential Refrigerants as Substitutes for R410A in Ground Source Heat Pumps. *Energies* **2019**, *12*, 3538. [[CrossRef](#)]
26. *Inter-Ministerial Decree of 26th June 2015. Application of Methodologies for the Energy Calculation and Definition of Prescriptions and Minimum Requirements for Buildings*; Ministero delle Imprese e del Made in Italy: Rome, Italy, 2022. Available online: <https://www.mimit.gov.it> (accessed on 15 June 2023). (In Italian)
27. TEES company, TRNSYS 18: A Transient System Simulation Program. Available online: <http://www.trnsys.com> (accessed on 15 June 2023).
28. Dongellini, M.; Morini, G.L. On-off cycling losses of reversible air-to-water heat pump systems as a function of the unit power modulation capacity. *Energy Convers. Manag.* **2019**, *196*, 966–978. [[CrossRef](#)]
29. *BS EN 13779-Ventilation for Non-Residential Buildings-Performance Requirements for Ventilation and Room-Conditioning Systems*; British Standards Institution (BSI): London, UK, 2007.
30. *ANSI/ASHRAE Standard 34-2019; Designation and Safety Classification of Refrigerants*; American Society of Heating, Refrigerating and Air-Conditioning Engineers Inc.: Atlanta, GA, USA, 2019.
31. *UNI EN 14825:2022; Air Conditioners, Liquid Chilling Packages and Heat Pumps, with Electrically Driven Compressors, for Space Heating and Cooling, Commercial and Process Cooling—Testing and Rating at Part Load Conditions and Calculation of Seasonal Performance*. UNI (Ente Italiano di Normazione): Rome, Italy, 2022.
32. *UNI EN 378-1:2021; Refrigerating Systems and Heat Pumps—Safety and Environmental Requirements—Part 1: Basic Requirements, Definitions, Classification and Selection Criteria*. UNI (Ente Italiano di Normazione): Rome, Italy, 2021.
33. Bjonness, K.L.; Gustafsson, T.; Ishikawa, J.; Maione, M. Emissions of Fluorinated Substitutes for Ozone Depleting Substances. In *2019 Refinement to the 2006 IPCC Guidelines for National Greenhouse Gas Inventories*; IPCC: Bern, Switzerland, 2019; Volume 3, p. 7.32. Available online: https://www.ipcc-nggip.iges.or.jp/public/2019rf/pdf/3_Volume3/19R_V3_Ch07_ODS_Substitutes.pdf (accessed on 15 June 2023).
34. ISPRA. 363/2022. *Efficiency and Decarbonization Indexes of the National Energy System and of the Electric Sector*; ISPRA: Rome, Italy, 2022. Available online: <https://www.isprambiente.gov.it/files2022/pubblicazioni/rapporti/r363-2022.pdf> (accessed on 15 June 2023). (In Italian)
35. Naldi, C.; Zanchini, E. A new numerical method to determine isothermal g-functions of borehole heat exchanger fields. *Geothermics* **2019**, *77*, 278–287. [[CrossRef](#)]
36. Emmi, G.; Zarrella, A.; De Carli, M.; Donà, M.; Galgaro, A. Energy performance and cost analysis of some borehole heat exchanger configurations with different heat-carrier fluids in mild climates. *Geothermics* **2017**, *65*, 158–169. [[CrossRef](#)]

Disclaimer/Publisher’s Note: The statements, opinions and data contained in all publications are solely those of the individual author(s) and contributor(s) and not of MDPI and/or the editor(s). MDPI and/or the editor(s) disclaim responsibility for any injury to people or property resulting from any ideas, methods, instructions or products referred to in the content.